Application of Nanocrystalline Silicon and Ballistic Electron Emitter to Flat Panel Display Devices

by N. Koshida, A. Kojima, Y. Nakajima, T. Ichihara, Y. Watabe, and T. Komoda

Because of a significant carrier-confinement effect, various remarkable properties are induced in quantum-sized nanocrystalline silicon (nc-Si).[1] A typical example is anodized porous silicon (PS), wherein the fundamental band dispersions of single-crystalline silicon (c-Si) are retained but the bandgap is significantly widened.[2] In addition to visible photoluminescence[3] and electroluminescence,[4] the PS device shows negative-resistance[5] and nonvolatile memory[6] due to strong electrical charging, cold electron emission based on high-field conduction,[7] thermally induced ultrasonic emission,[8] and biodegradability related to enhanced surface activity.[9]

As reported previously,[7, 10-12] a nanocrystalline PS diode composed of a thin Au film, nanocrystalline PS, a Si substrate, and an ohmic back contact emits uniformly electrons under a biased condition. In accordance with analyses of the electron emission characteristics, the emission mechanism is based on a specific field-induced electron drift in the PS layer associated with generation of hot electrons and the subsequent ejection via tunneling through the top contact. In contrast to the case of conventional field emitter arrays, the acceleration process in the PS layer is a key factor for the efficient emission. In fact, the PS diode formed on n^+-Si substrates with a controlled nanostructure operates as an efficient surface-emitting ballistic electron source.[13] This cold cathode can also be fabricated based on nanocrystallized porous polycrystalline silicon (nc-PPS) films as well.[14,15] As one of the possible applications, a prototype full-color ballistic electron surface-emitting display (BSD) has been developed on glass substrates.[16-18] The present article describes the fundamental characteristics of this emitter and some evidence for the ballistic emission model. The advantageous features as a cold cathode and the technological potential are also presented.

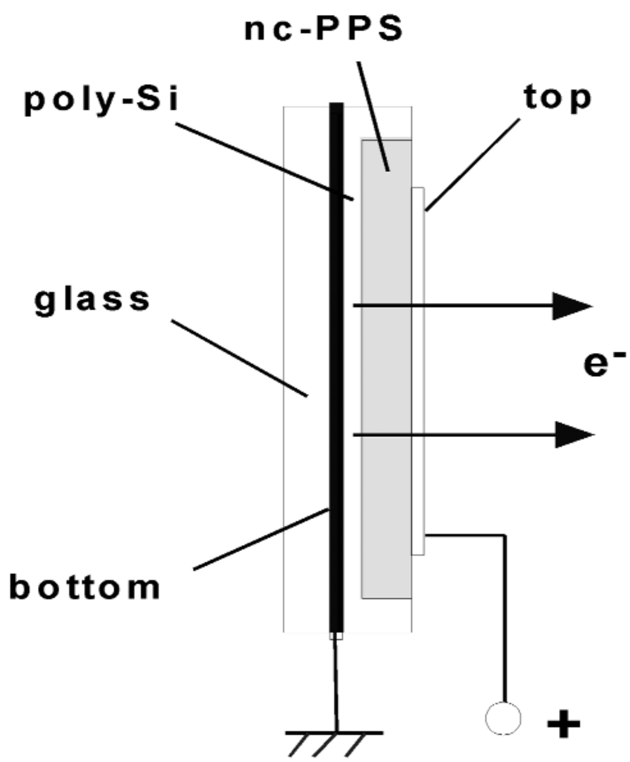

FIG. 1. Schematic of poly-Si-based cold cathodes formed on a glass substrate. The deposited poly-Si films are anodized to produce nc-Si layers followed by rapid thermal oxidation (RTO) or electrochemical oxidation (ECO) treatment.

Cold Cathode Production

The cold cathodes are fabricated on c-Si substrates or 1.5 µm thick polycrystalline Si (poly-Si) films formed by low-pressure or plasma-enhanced chemical vapor deposition (LPCVD or PECVD) method on c-Si substrates. In the case of c-Si substrates, the device is composed of a thin Au film (10 nm in thickness), a 3-10 µm thick PS layer treated by rapid thermal oxidation (RTO) at 900-1000°C or electrochemical oxidation (ECO) in a 1N H_2SO_4 solution for a few minutes, an n^+-type Si(111) wafer, and an ohmic back contact. The PS or PPS layer is formed by conventional galvanostatic photoanodization in an ethanoic HF solution at a constant temperature. The post-anodization RTO or ECO treatment is useful for enhancing the field effect.

To make the generation of hot and ballistic electrons more efficient, the anodization current modulation technique is employed such that the multilayer or graded-band multilayer structure is formed. Similar processing is applied to the poly-Si films deposited on glass substrates. As a typical example of the fabricated device, a schematic of cross-sectional views of poly-Si film-based cold cathodes formed on a glass substrate is shown in Fig. 1.

The characteristics of the device are measured in a demountable ultra-high-vacuum (UHV) system in terms of the applied voltage (V_{PS}) dependence of the diode current J_{PS} and electron emission current J_e. To investigate the emission mechanism, the energy distribution curves of emitted electrons are measured by a conventional ac-retarding potential method as a function of V_{PS} and temperature. The electron transport in the PS layer can also be investigated using a time-of-flight technique. For this measurement, a short pulse UV

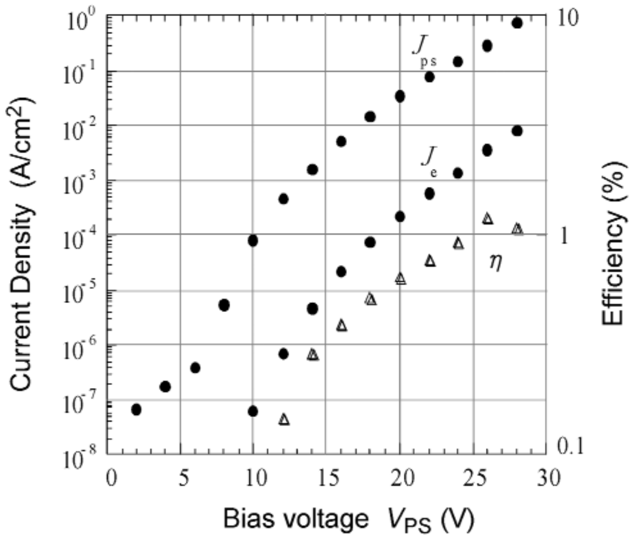

FIG. 2. The current-voltage (J_{PS}-V_{PS}) characteristics of a nc-PPS diode fabricated on a glass substrate and the corresponding electron emission current J_e characteristics. The emission efficiency η defined as the ratio J_e/J_{PS} is also shown.

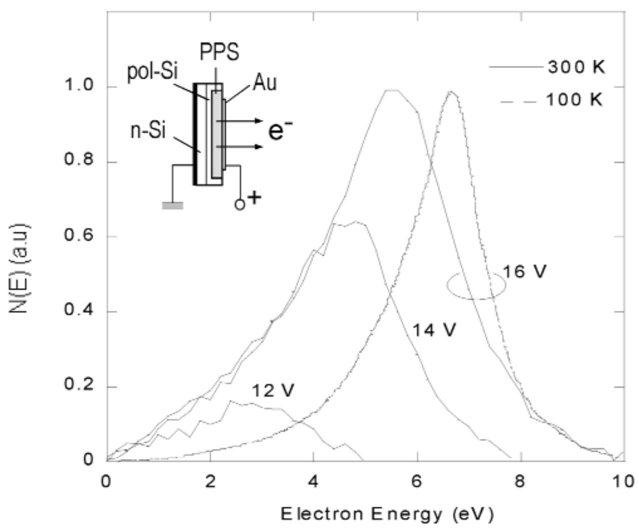

FIG. 3. The energy distribution curves of electrons emitted from a porous polycrystalline silicon (PPS) diode at different applied voltages at room and low temperatures. The schematic cross section of the device is also shown. The PPS layer was prepared by photoanodizing a non-doped poly-Si film (1.5 µm thick) deposited onto an n^+-type (100) Si wafer.

laser (35 ps in width) is used for exciting one side of the self-supporting samples under a biased condition. The PS films are obtained by an electrochemical peeling from the substrate. The average drift length of electrons in the PS layer at different V_{PS} is obtained from analyses of observed transient photocurrent curves at room and low temperatures.

The usefulness of the ballistic PS cold cathode as an excitation source of a fluorescent screen has been investigated for a vacuum-type flat panel device. Operability for a simple matrix operation without any focusing electrodes between the device surface and the screen has been confirmed by construction of a 2.6-inch full-color dynamic image display. It demonstrates that ballistic electrons generated in the PS layer are utilized directly for excitation of fluorescent films formed on the PS surface without ejecting into the vacuum.

Emission Characteristics and Mechanism

When a positive bias voltage is applied to the top contact with respect to the substrate, electrons are efficiently and uniformly emitted through the surface electrode. Figure 2 shows J_{PS} and J_e as a function of V_{PS} for a PPS device. The emission current with an onset voltage of 6 V is rapidly increased with increasing V_{PS}. The J_e reaches 8 mA/cm^2 at V_{PS} = 28 V. The corresponding efficiency defined as a ratio and J_e/J_{PS} is beyond 1%. This emission is presumably caused by a field-induced tunnel effect, since Fowler-Nordheim plots obtained from V_{PS}-J_e curves follow a linear behavior.

During anodization of poly-Si films, nc-Si particles are preferentially produced at the grain boundaries. The residual silicon grains (about 100 nm diameter in this case) act as a heat sink to suppress local heating. So there are little spike-like fluctuations in the time evolution of both J_{PS} and J_e. From a technological viewpoint, the availability of poly-Si films is very important for large-area applications. Another important feature is that the emission current is insensitive to vacuum pressure. Similar stability was also observed in the diodes fabricated on c-Si substrates with a multilayer and graded-band multilayer PS structures.

When an electric field is applied to the PS or PPS diode in which nc-Si particles are interconnected via thin oxide films, most of the potential drops should be produced only at the interfacial barriers between neighboring nc-Si particles, and then the extremely high electric field is periodically generated along the depth direction. Because of concentrated equipotential lines, the electric field strength at the contact area becomes considerably higher than that in the case of planar structure. Under this situation, electrons injected into the PS layer can travel for a long distance via multiple-tunneling through thin oxide interfacial layers. As a result of this cascade acceleration, hot or ballistic electrons are efficiently generated. Due to obtaining sufficient kinetic energy, electrons at the outer surface region are easily emitted into the vacuum by tunneling through the thin Au film. In this situation, the emission efficiency should not be strongly dependent on the barrier height at the top contact. This is consistent with the insensitivity of the emission current to the vacuum pressure.

This hypothesis is supported by the experimental data for the energy distribution of emitted electrons. The energy distribution of emitted electrons is determined from the product of the electron population and the tunneling probability. As indicated in Fig. 3, the observed energy distribution curve is totally different from the thermalized Maxwellian type. Both the peak and mean energies shift towards the higher energy side in accordance with increasing bias voltages. At low temperatures below 150 K, wherein the tunneling conduction mode is dominant, electrons are accelerated without significant scattering losses. So the energy spread becomes quite small due to a significant reduction of the low-energy tail component, as indicated by the dashed curve in Fig. 3.

Other evidence has been provided by a electron transport analysis based on time-of-flight (TOF) measurements for a self-supporting PS film.[19] The transient TOF signal shows a simple exponential decay, which is different from the behavior of both c-Si and hydrogenated amorphous silicon. The decay time constant is independent of applied voltage. The implication is that electrons travel in PS with a certain trapping rate. From analyses of the observed TOF signals, the electron mean free path L_e can be determined. The L_e value obtained shows a strong field dependence and reaches 1.6 µm for an electric field of $3x10^4$ V/cm even at room temperature. At a low temperature of 100 K, the L_e value is higher than 2 µm. These lengths are hundreds of times larger than the mean size of nc-Si in PS. The average kinetic energies estimated from this result are consistent with the observed energy distribution of emitted electrons shown in Fig. 3.

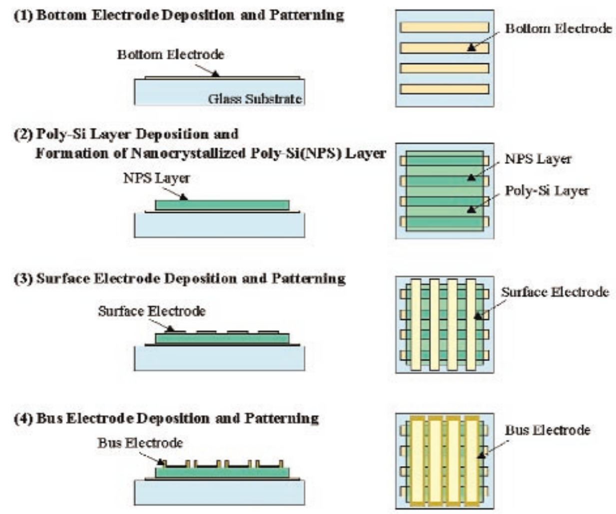

FIG. 4. Processing steps for fabrication of ballistic surface-emitter arrays. The nanocrystalline poly-Si emitter arrays are formed on a glass substrate.

(a)

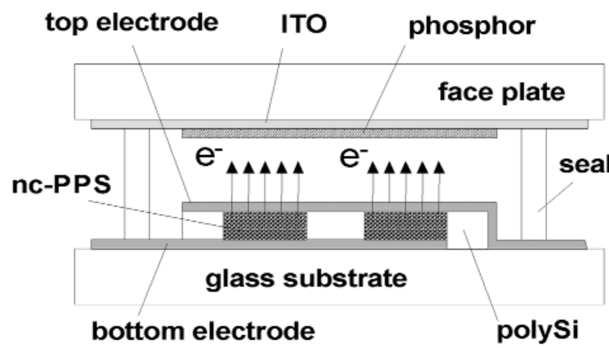

(b)

FIG. 5. A schematic cross sectional structure of a full-color nc-PPS display device fabricated on a glass substrate (a) and the corresponding emission image (b). Note that there are no focusing electrodes between the device and the phosphor screen. Device parameters are as follows: size: 2.6 inches in diagonal; pixel: 128(RGB)x126 pixels; pixel pitch: 50 µm; vacuum spacing: 3.5 mm; accelerating voltage: 5 kV; driving: simple matrix mode.

Possible Applications

This PS-based ballistic electron emitter has the following advantageous features over the conventional field-emitter and other cold cathodes: (1) surface-emitting capability; (2) low-voltage operation; (3) insensitivity to vacuum pressure; (4) energetic electron emission; (5) small emission angle dispersion; (6) quick response; (7) availability for large-area devices; and (8) compatibility with silicon planar processing as illustrated in Fig. 4.

Based on these advantages, many applications can be pursued. One promising approach is the use for a vacuum-type flat panel display.[19] In Fig. 5a, a schematic is shown of the PPS emitter display device produced on a glass substrate. Using this emitter as an excitation source of a fluorescent screen placed at a spacing of 3.5 mm from the device surface, a simple-matrix full-color flat panel display has been developed without any focusing electrodes. The emission image pattern of a proto-type simple-matrix 2.6 inches display of a 168(RGB)x126 pixels with a 50 µm pitch as shown in Fig. 5b. Due to the energetic and collimated electron emission perpendicular to the device surface, the emission image shows no significant cross-talk despite the lack of any focusing systems. The device also shows a sufficient performance for dynamic image display. Further development for a large-area flat-panel display with higher resolutions is in progress using a low-temperature processing suitable for thin-film-transistor or plasma-display compatible glass substrates.

As indicated in Fig. 3, energetic electrons are efficiently generated in the PS layer and their mean kinetic energies can be controlled by an external applied voltage. This makes it possible to utilize those electrons in the diode without ejecting into the vacuum, as shown in Fig. 6. In this case, an organic

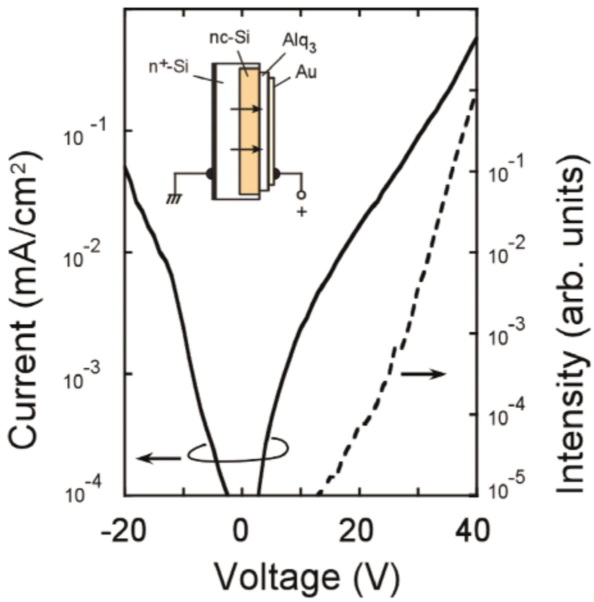

FIG. 6. Schematic structure of a fabricated solid-state light-emitting device based on ballistic electron excitation (inset), the current-voltage characteristics and the corresponding luminescence intensity (the dashed curve).

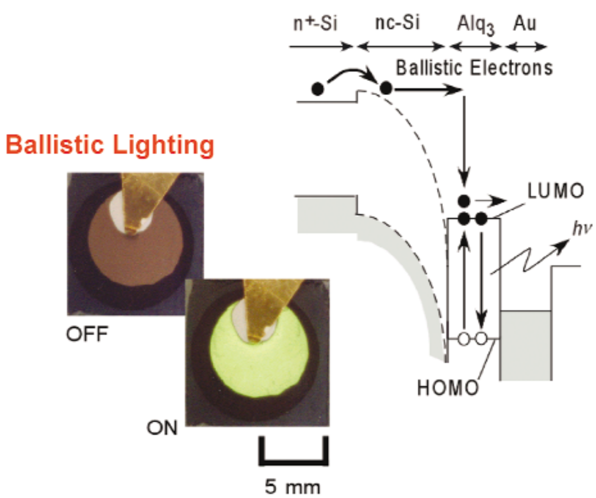

FIG. 7. Photograph of a ballistic lighting device at off and on states. Energetic electrons generated in the nc-Si layer directly excite the fluorescent film (an organic material in this case). Uniform bright green emission is observed through the top contact at an applied forward bias voltage of 25 V.

luminescent film (Alq_3: tris (8-hydroxyquinoline) aluminum in this case) is deposited onto the PS layer surface by vacuum evaporation as a fluorescent screen. Under a positive bias voltage, generated hot and quasi-ballistic electrons should directly excite the luminescent film and produce visible light. This can be regarded as a solid-state cathodoluminescence.

Typical current-voltage characteristics and the corresponding luminescence intensity are shown in Fig. 5.[20] A uniform green luminescence is observed only in the positive bias region with an onset voltage of 12 V. The light emission from a graded-multilayer PS structure device is significantly more efficient in comparison to that from a normal PS structure device prepared under a constant anodization current. Obviously, efficient generation of ballistic electrons in the nanocrystalline PS layer is a key issue for efficient operation. The light emission at a voltage of 25 V is clearly discernible in the daylight. Photographs of the device at the off- and on-states are shown in Fig. 6. Uniform green light is emitted from the whole active area of a semitransparent thin Au film with neither local bright spots nor fluctuations. Similar results were also obtained from the devices based on anodized poly-Si films.[21] Both the observed peak wavelength and bandwidth of emission spectra, which coincide well with those of the original ones of the deposited material, are independent of the applied voltage. In addition to organic materials, inorganic ones are available for the fluorescent films of this device. These experimental facts support the hypothesis of luminescence based on the ballistic electron excitation scheme. This ballistic lighting device should be applicable to a large-area visible light source and high-quality vacuum-less flat panel display.

Conclusions

It has been shown that a structure-controlled nanocrystalline PS layer is useful as an electron drift layer to generate hot and ballistic electrons. The experimental results suggest that there is a characteristic field-induced electron transport mode in an interconnected nc-Si system. Based on this effect, an efficient planar cold cathode has been developed. This emitter has many advantageous features for practical uses. One possible application is an excitation source for a vacuum-type flat panel display. The generation of energetic electrons is also directly applicable to a novel solid-state surface-emitting light source. ■

Acknowledgements

This work was partially supported by a Grant-in-Aid from the Ministry of Education, Culture, Sports, Science and Technology of Japan and from the Japan Science and Technology Corporation (CREST Program).

References

1. N. Koshida and N. Matsumoto, *Mater. Sci. & Eng. R,* **40**, 169 (2003).
2. Y. Suda, K. Obata, and N. Koshida, *Phys. Rev. Lett.,* **80**, 3559 (1998).
3. L. T. Canham, *Appl. Phys. Lett.,* **57**, 1046 (1990).
4. N. Koshida and H. Koyama, *Appl. Phys. Lett.,* **60**, 347 (1992).
5. K. Ueno, H. Koyama, and N. Koshida, *Jpn. J. Appl. Phys.,* **37**, 1096 (1998).
6. K. Ueno and N. Koshida, *Appl. Phys. Lett.,* **74**, 93 (1999).
7. N. Koshida, T. Ozaki, X. Sheng, and H. Koyama, *Jpn. J. Appl. Phys.,* **34**, L705 (1995).
8. H. Shinoda, T. Nakajima, M. Yoshiyama, and N. Koshida, *Nature*, **400**, 853 (1999).
9. L. T. Canham, *Adv. Mater.,* **7**, 1033 (1995).
10. X. Sheng, T. Ozaki, H. Koyama, and N. Koshida, *J. Vac. Sci. & Technol. B,* **15**,1661 (1998).
11. X. Sheng, H. Koyama, and N. Koshida, *J. Vac. Sci. & Technol. B,* **16**, 793 (1998).
12. X. Sheng and N. Koshida, *Mat. Res. Soc. Symp. Proc.,* **509**, 193 (1998).
13. N. Koshida, X. Sheng, and T. Komoda, *Appl. Surf. Sci.,* **146**, 371 (1999).
14. T. Komoda, X. Sheng, and N. Koshida, *J. Vac. Sci. & Technol. B,* **17**, 1076 (1999).
15. X. Sheng, A. Kojima, T. Komoda, and N. Koshida, *J. Vac. Sci. & Technol. B,* **19**, 64 (2001).

16. T. Komoda, Y. Honda, T. Hatai, Y. Watabe, T. Ichihara, K. Aizawa, Y. Kondo, and N. Koshida, Society of Information Display, *Digest of Technical Papers,* **Vol. 31**, p. 428, SID, San Jose, CA (2000).
17. T. Komoda, Y. Honda, T. Hatai, Y. Watabe, T. Ichihara, K.Aizawa, and N. Koshida, Society of Information Display, *Digest of Technical Papers,* **Vol. 32**, p. 14-1, SID, San Jose, CA (2001).
18. T. Komoda, Y. Honda, T. Ichihara, T. Hatai, Y. Takegawa, Y. Watabe, K. Aizawa, V. Vesin, and N. Koshida, Society of Information Display, *Digest of Technical Papers,* **Vol. 33**, p. 1128, SID, San Jose, CA (2002).
19. A. Kojima and N. Koshida, *Jpn. J. Appl. Phys.,* **41** (2003) (in press).
20. Y. Nakajima, A. Kojima, and N. Koshida, *Appl. Phys. Lett.,* **81**, 2472 (2002).
21. Y. Nakajima, H. Toyama, A. Kojima, and N. Koshida, *Jpn. J. Appl. Phys.,* **41**, 2707 (2002).

About the Authors

Nobuyoshi Koshida *is a Professor in the Department of Electrical and Electronic Engineering at Tokyo University of Agriculture and Technology (TUAT). He is the chairman of the Japan Section of ECS. He may be reached by e-mail at koshida@cc.tuat.ac.jp..*

A. Kojima *is with Quantum 14 Co., in Tokyo, Japan. He may be reached by e-mail at kojimaa@cc.tuat.ac.jp.*

Y. Nakajima *is with the Department of Electrical and Electronic Engineering at Tokyo University of Agriculture and Technology. He may be reached by e-mail at nakajm@cc.tuat.ac.jp.*

T. Ichihara *is with the Matsushita Electric Works Co., in Osaka, Japan. He may be reached by e-mail at ichihara@crl.mew.co.jp.*

Y. Watabe *is with the Matsushita Electric Works Co., in Osaka, Japan. He may be reached by e-mail at wata@crl.mew.co.jp.*

T. Komoda *is with the Matsushita Electric Works Co., in Osaka, Japan. He is also a visiting professor at TUAT. He may be reached by e-mail at komoda@crl.mew.co.jp.*